

See discussions, stats, and author profiles for this publication at: <https://www.researchgate.net/publication/243970011>

A novel algorithm for damage analysis of fatigue sensor by surface deformation relief parameters

Conference Paper · May 2013

CITATIONS

9

READS

104

5 authors, including:



[Sergey Ignatovich](#)

National Aviation University

55 PUBLICATIONS 83 CITATIONS

[SEE PROFILE](#)



[Abdellah Menou](#)

Académie Internationale Mohammed VI de l'Aviation Civile, Casablanca, M...

45 PUBLICATIONS 184 CITATIONS

[SEE PROFILE](#)

Some of the authors of this publication are also working on these related projects:



Surface relief as an indicator of accumulated fatigue damage [View project](#)



The effect of operational factors on the loss of plasticity, degradation of structure, crack resistance of materials in main pipelines after long service [View](#)

All content following this page was uploaded by [Sergey Ignatovich](#) on 05 June 2014.

The user has requested enhancement of the downloaded file.



ISORAP 2013

INTERNATIONAL SYMPOSIUM

OPERATIONAL RESEARCH AND APPLICATIONS

EDITORS :

A. MENOU, M. WAKRIM, A. MOUDDEN, M. BENADDY

MAY 08 -10, 2013 MARRAKECH MOROCCO

ISORAP 2013

**INTERNATIONAL SYMPOSIUM
ON OPERATIONAL RESEARCH AND APPLICATIONS**

Dépôt Légal : 2013 MO 1475
ISBN : 978 - 9954 - 32 - 222 - 2

ISORAP 2013





ISORAP2013

Organizing Committee

Chairman	Co-Chairman
Abdellah Menou Mohammed VI AIAC, Morocco	Younes CHAHLAOUI King Khalid University,KSA/University of Manchester,UK Mohamed Wakrim, Ibn Zohr University, Agadir Morocco
	Members
	Ali Mouden, Ibn Zohr University, Agadir Morocco Imad IMMAS, Morocco Mohamed Mansouri, Hassan 1 University, Settat Morocco Bouchaib Radi, Hassan 1 University, Settat Morocco Rachid Alaoui, High School of Technology Agadir Morocco Mohamed Benaddy, Faculty of Sciences Agadir Morocco



ISORAP2013

Scientific and steering committee

Løkketangen Arne, Molde University College, Molde, Norway
Javier Alcaraz , Universidad Miguel Hernández De Elche, Alicante, Spain
Mustapha Amghar, GIE Galileo, Rabat, Morocco
Ryosuke Ando, Toyota Transportation Research Institute , Japan
Noureddine Barka, University of Quebec at Rimouski, UQAR, Canada
Abderrazak El Ouafi, University of Quebec at Rimouski, UQAR, Canada
Mohamed Benbouziane, MIFMA, University of Tlemcen, Algeria
John Boland, Barbara Hardy Inst. and Scho. of Math. and Statistics, University of South Australia
Xiaoqiang Cai, Chinese University of Hong Kong (Cuhk), China
Younes CHAHLAOUI, University of Manchester, UK/ King Khalid University, KSA
Joao Climaco, University of Coimbra, Coimbra, Portugal
Demange Marc, ESSEC Business School, Paris , France
Duan Li, Chinese University of Hong Kong, Hong Kong, China
Zari Dzalilov University of Ballarat, Ballarat, Australia
Xuexiang Huang, Chongqing University, Chongqing, China
Nawal El Assasi, European Central Bank, Frankfurt, Germany
Babek Erdebili, Atılım University, Incek/Ankara, Turkey
Chang Jung, Christian University, Taiwan
Zopounidis Konstantinos , Technical University of Crete, Greece
Risto Lahdelma, Aalto University, Department of Energy Technology, Finland
Lakatos László, Eotvos Lorand University, Budapest, Hungary
Luhandjula Jean-Pierre, University of South Africa, South Africa
Stella Sofianopoulou, University of Piraeus, Greece
Luiz Autran Gomes, Ibmecc/RJ, National Academy of Engin, Rio de Janeiro, Brazil
Fernando A. S. Marins, Universidade Estadual Paulista, Guaratinguetá/ São Paulo – Brasil
Yu Mei, University of International Business and Economics , Beijing, China
Abdellah Menou, International Academy of Civil Aviation, Casablanca, Morocco
Pavlo Maruschak, Ternopil Ivan Pul'uj National Technical University, Ukraine
Alper E. Murat, Department of Industrial and Systems Engineering, Wayne State University, USA
Dr. Sharafali Moosa, Singapore Management University, Singapore
Sundaravalli Narayanaswami, Higher Colleges of Technology, Abu Dhabi, UAE
Yurii NESTEROV, Catholic University of Louvain (UCL), Belgium
Andy Philpott, University of Auckland, Auckland, New Zealand
Abdelaziz Rhandi, University of Salerno, Salerno, Italy
Ruiz-Hernandez, CUNEF, Madrid, Spain
Saverio Salerno, University of Salerno, Italy
Roman Slowinski, Poznan University, Poznan, Poland
Tatjana Tambovceva, Riga Technical University, Latvia
Cerasela Tanasescu, Essec, Paris, France
Jacques Teghem, University of Mons, Mons, Belgium
Jozsef Temesi, Corvinus University of Budapest, Hungary
OTomáš Tichý, VŠB-Technical University of Ostrava, Czech Republic
Ayhan Ozgur Toy, Istanbul Bilgi University, Turkey
Nico Vandaele, Faculty of Business and Economics, Belgium
Mohamed Wakrim, Mathematical Department, Ibn Zohr University, Agadir, Morocco
Weiqi Li, University of Michigan-Flint, USA
Farouk Yalaoui , UTT, France

IX Materials and Process Session 649

Experimental study of springback due to the stretch-bending operation applied to titanium (T40) sheet metals	651
Etude numérique du comportement des assemblages en acier par plat soude d'extrémité	659
Reliability Assessment of Underground Pipelines Under Active Corrosion Defects	666
A novel algorithm for damage analysis of fatigue sensor by surface deformation relief parameters	674
Interface Capturing between Two Phases for Pelton Turbine Injector Using a Velocity Method	681
Influence d'un Effet Corrosif sur les Performances Mécaniques d'un Acier API 5L X70	695
Reliability Analysis of Plate Hydroforming Process based Metamodels	702
Simulation numérique de la rigidité à la flexion des aubes vrillées longues et extra longues des turbines à vapeur	703
Applications of Viscoelastic Eshelby-Kröner self-consistent model: Multi-scale behavior of polymer composites under creep loading	710
Finite element modeling and numerical simulation of aeroacoustic problem with deterministic and probabilistic approaches	716
Résolution des équations de Navier Stokes bidimensionnelles en Régime Laminaire Supersonique par la méthode de McCormack	723
Effet de la Température Totale et de Nombre de Mach sur l'Onde de Choc Oblique à haute température	735
Elastic plastic analysis of bonded composite repair in cracked aircraft structures	743
Modélisation des stratégies de commande appliquées aux différentes zones de fonctionnement d'une éolienne	744

X UQAR Posters Session 749

An interactive multiple-objective optimisation based decision making for machine setup in metal cutting operations	751
Simulation of Spline Heated by Scanning Induction - 3D Model	752
Optimization of hardness profile of 4340 Steel Specimen Heated by Induction Process Using Axi-symmetric Simulation	753
Hybrid optimisation design approach for electromagnetic devices - application for eddy current brake design	754

XI Materials and Process Posters Session 755

Apport de la phase pour la localisation des résonances acoustiques diffusées par le cylindre élastique en incidence oblique	757
Résolution des problèmes inverses par la méthode de gradient conjugué pour identifier les paramètres thermiques d'un matériau	759
Reliability analysis and numerical modeling of vibroacoustic problems of complex structures	762
Seismic vulnerability assessment of Moroccan reinforced concrete buildings using pushover analysis	770
Estimating the permeability of macroporous soil susceptible to erosion macroporous treated by the slag	777

A novel algorithm for damage analysis of fatigue sensor by surface deformation relief parameters

[†]I. Konovalenko, [†]P. Maruschak, ^{*}A. Menou, ^{**}M. Karuskevich, ^{**}S. Ignatovich

[†]Ternopil Ivan Pul'uj National University,
Ruska 56, Ternopil, 46001, Ukraine, E-mail: laboratory22b@gmail.com

^{*}International Academy of Civil Aviation
Casa-Mohammed Airport

^{**}National Aviation University,
Komarova ave. 1, Kiev 03680, Ukraine

Abstract

Fatigue damage of metal structures may be estimated by the application of sensors with the surface relief pattern indicating the accumulated fatigue damage. The nature of the deformation relief has been investigated. Digital analysis of the surface patterns based algorithm for the integral evaluation method has proved the efficiency of integral parameters (the general area of damage, mean gradient along the coordinate axes, and the mean amplitude of the histogram function spectrum) application for additional quantitative description of such surface structures. The evolution of deformation relief parameters on the sensors surface is determined by the process of the sensor and construction fatigue damage accumulation.

1. Introduction

It is known that physical mesomechanics considers the surface layers of the material under loading as the independent subsystem highly sensitive to damage accumulation [1]. This was the reason for the development and use of fatigue sensors, which allow obtaining information about the relief, and which are used intensively in military and civil aviation. One of the advantages of such sensors is that they allow getting the physically grounded information, which can be used both during operation and preventive inspections after certain periods of service [2]. Moreover, the acquisition of such information is the basis for the creation of models for predicting the accumulation of damage and nucleation of microdefects.

3D stochastic models of stress and strain distribution on the polycrystal surface are known, which substantiate theoretically the special role of the surface layer in hard bodies under loading, as well as the development of the non-linear undulatory processes in them at the meso- and macrolevels [3]. Such methods allow calculating the distribution of normal and tangential stresses in the surface layers, and on the internal boundaries of the material. The practical value of this consists in the possibility to perform digital modeling of the fatigue sensor condition.

Contemporary profilometry methods allow for the functional diagnostics of the surface condition and recording the morphological parameters of structural formations. However, the

development of the effective approaches to the identification, analysis and generalisation of the obtained data about the surface damage remains topical [4].

The purpose of this work is to develop the algorithm for evaluating the fatigue damage of the foil sensor as the nonlinear hierarchically organised structural-mechanical system, which allows for the calculation of the integral quantitative characteristics based on the analysis of the photo image of the deformation relief.

2. Algorithm for calculation of deformation relief parameters

A foil sensor was fixed on the specimen from alloy D16AT, which was tested under maximum loading of the zero-to-tension stress cycle $\sigma_{\max} = 180.0$ MPa with the loading frequency of 11.0 Hz [2]. The elementary act of plastic yielding during the accumulation of fatigue damage in the material was the “shear + turn” of structural elements. This caused the appearance of dissipative mesostructures and the accumulation of fatigue damage on fatigue sensors.

The surface relief parameters of the polycrystalline aluminum fatigue sensor were calculated by means of analysis of the initial photo image (Fig.1,a) $I_0(x,y)$. The algorithm consists of two stages. The first stage, the preparatory one, consists of operations that include equalisation of the illumination, filtering, binarisation, and determining the slope angle. During the second stage, the quantitative integral characteristics, which allow evaluating the general condition of the specimen, were calculated by means of analysis of the obtained image.

Preliminary image processing. The image illumination was equalised in order to eliminate the effect of the shaded areas in the initial image on the work result. This operation was performed by folding the image with the low-frequency filter followed by the removal of the low-frequency component.

The Gaussian filter with quite a large kernel size was used for filtration, the result of which was the obtained approximate image of illumination $I'(x, y)$ (where x is the column index, $x \in (1..m)$; y is the row index I_0 , $y \in (1..n)$).

After that we obtained the image with the equalised illumination:

$$I_L(x, y) = K_L \cdot \frac{I_0(x, y)}{I'(x, y)}, \quad (1)$$

where $K_L = \max(I'(x, y))$ is the illumination equalisation coefficient.

In order to remove minor noise elements from the obtained image, which are caused by the peculiarities of the photomatrix operation, the median filter was used. It was realised with help of the filter, whose window points are sorted in ascending order, and the value in the middle of the ordered list is taken as the initial one. As a result of processing we obtain image I_f .

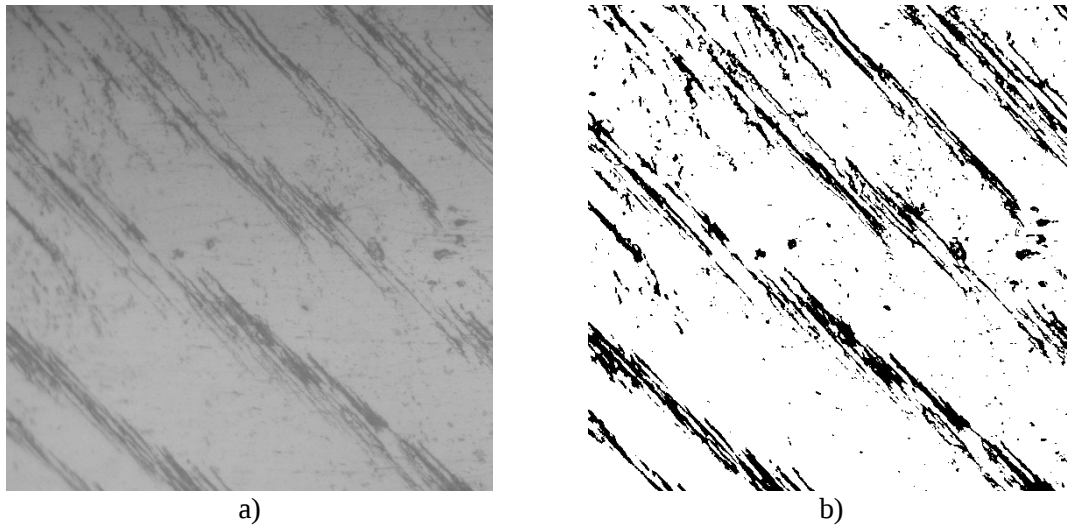


Figure 1: Initial grayscale image (a) and final binary image (b) of the polycrystalline aluminum fatigue sensor surface subjected to 40000 loading cycles

After the preliminary processing and improvement of the initial I_0 image quality the image was segmented. The purpose of segmentation was to distinguish the informative pixels (points of interest) in the image, which correspond to the deformation relief zones. Segmentation was performed using binary transformation. To this end, the limit I_{Blim} value was found in the histogram of the image brightness, which separates the background pixels from the informative pixels.

As a result of the above operations the binary I image was obtained (Fig. 1,b), in which black pixels (informative ones) correspond to the deformation relief elements, and white ones – to the background.

The deformation relief on the surface of the polycrystalline aluminum fatigue sensor is characterised by numerous linear fragments (Fig. 1). In order to obtain the quantitative integral indicators of such images [5] it is necessary to have the coordinate system, one axis of which repeats the propagation direction of linear fragments.

Turn of coordinate axis. The propagation direction of linear fragments of the deformation relief was determined using the Hough transformation, which consists in determining the compliance matrix between the image and the parameter space of straight lines (Duda and Hart, 1972). We assume that the family of straight lines in the plane is given by the parametric equation

$$h(\theta, \rho, x, y) = x \cdot \cos \theta + y \cdot \sin \theta - \rho, \quad (2)$$

where (x, y) is the parameter space of image I ; (θ, ρ) is the parameter space of the family of straight lines in the image (θ, ρ are the components of the normal equation for the straight line).

In the Hough transformation we calculate the matrix of S accumulators in the space of parameters (θ, ρ) with discreteness $\Delta\theta, \Delta\rho$ (in practice, during the analysis of images (Fig. 1) it was assumed that $\Delta\theta=1^\circ, \Delta\rho=4$ pixels). An accumulator with a certain number of informative points in the image corresponds to every cell of the phase space. The condition of belonging of point $i(x, y)$ in image I to straight line h , which is represented by the cell of parameter space $S(\theta, \rho)$, was accepted as follows:

$$r(x, y, \theta, \rho) = \begin{cases} 1, & \text{if } d(i(x, y), h(\theta, \rho, x, y)) \leq d_{\text{lim}} \\ 0, & \text{if else} \end{cases}, \quad (3)$$

where $d(i(x, y), h(\theta, \rho, x, y))$ is the distance from point $i(x, y)$ to straight line $h(\theta, \rho, x, y)$; d_{lim} is the limit value.

Thus, the Hough transformation function has the following view:

$$H(S(\theta, \rho)) = \sum r(x, y, \theta, \rho). \quad (4)$$

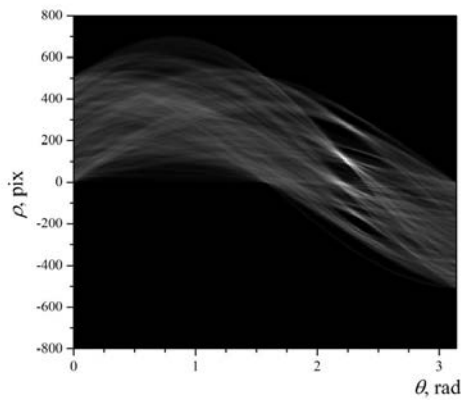


Figure 2: View of function $H(S(\theta, \rho))$ for deformation relief formations

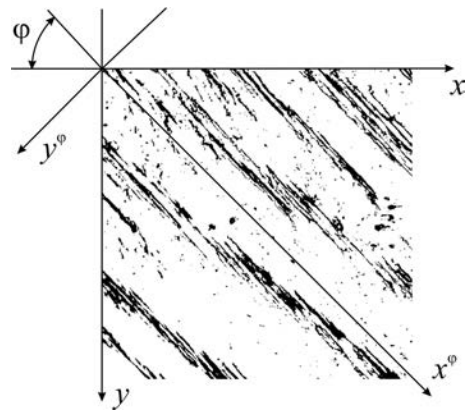


Figure 3: Turn of coordinate system of the image in the propagation direction of deformation relief elements

The quantitative analysis of accumulators in the parameter space allows finding straight lines in the image with the greatest number of informative points. The zones, in which function $H(S(\theta, \rho))$ attains maxima, correspond to the most clearly defined straight lines. The relevant value of parameter $\theta = \theta_{\text{base}}$ characterises the predominant direction of propagation of the informative points (deformation relief elements). The view of function $H(S(\theta, \rho))$ for image (Fig. 1,b) is shown in Fig. 2.

Next we consider image I in coordinate system (x^φ, y^φ) , which is turned relative to the beginning of coordinate axis (x, y) by angle $\varphi = \theta_{\text{base}} - \frac{\pi}{2}$ (Fig. 3). For the image shown in Fig 1,b, angle $\theta_{\text{base}} = 2.30 \text{ rad} = 132^\circ$.

3. Parameters of quantitative evaluation of relief elements

For the purpose of the quantitative evaluation of the deformation relief condition on the test specimen surface a number of parameters were used, which were calculated based on the analysis of the processed grayscale image I_f and binary image I .

For every pixel in image I_f the absolute value of the horizontal and vertical gradient was calculated:

$$\nabla I_f^h(x^\varphi, y^\varphi) = \left| \frac{\partial I_f(x^\varphi, y^\varphi)}{\partial x^\varphi} \right|, \quad \nabla I_f^v(x^\varphi, y^\varphi) = \left| \frac{\partial I_f(x^\varphi, y^\varphi)}{\partial y^\varphi} \right|. \quad (5)$$

In order to generalise the evaluation of the investigated surface condition the mean values of the horizontal and vertical gradients of the image were used:

$$G_h = \overline{\nabla I_f^h} = \frac{1}{S_I} \iint \nabla I_f^h(x^\varphi, y^\varphi) dx^\varphi dy^\varphi, \quad G_v = \overline{\nabla I_f^v} = \frac{1}{S_I} \iint \nabla I_f^v(x^\varphi, y^\varphi) dx^\varphi dy^\varphi, \quad (6)$$

(6)

where $S_I = mn$ is the image area.

The gradient allows for the quantitative evaluation of the non-uniformity degree of the surface analysed along the coordinate axes [6]. A low mean value of the gradient testifies to an insignificant change in the intensity along the given axis of the image. In practice this means the uniform picture of the ordered structures in a certain direction [7] and points to the coordinate axis, which corresponds to the prevailing direction of the defect propagation.

The most general informative parameter, which allows evaluating the specimen damage by the obtained image, is the relative area of morphological formations:

$$S_d = \frac{S}{m \cdot n} \cdot 100\%, \quad (7)$$

where S is the number of pixels of the ordered structures in image I .

The distribution of the ordered structure elements along axes (x^φ, y^φ) of the image is described by vertical H_v and horizontal H_h histograms [8]:

$$H_h(y^\varphi) = \sum_{x^\varphi=1}^{m\varphi} I(x^\varphi, y^\varphi), \quad H_v(x^\varphi) = \sum_{y^\varphi=1}^{n\varphi} I(x^\varphi, y^\varphi), \quad (8)$$

where $m\varphi, n\varphi$ are the image dimensions in the coordinate system (x^φ, y^φ) along axes x^φ and y^φ , respectively.

Since after the turn of the coordinate system the image cross-section becomes different for different values x^φ (or y^φ), the histograms were normalised to make possible the comparative analysis:

$$H_h^n(y^\varphi) = \frac{H_h(y^\varphi)}{d_I(y^\varphi)} \cdot 100\%, \quad H_v^n(x^\varphi) = \frac{H_v(x^\varphi)}{d_I(x^\varphi)} \cdot 100\%, \quad (9)$$

where $d_I(y^\varphi), d_I(x^\varphi)$ are the image dimensions for coordinates y^φ and x^φ , respectively.

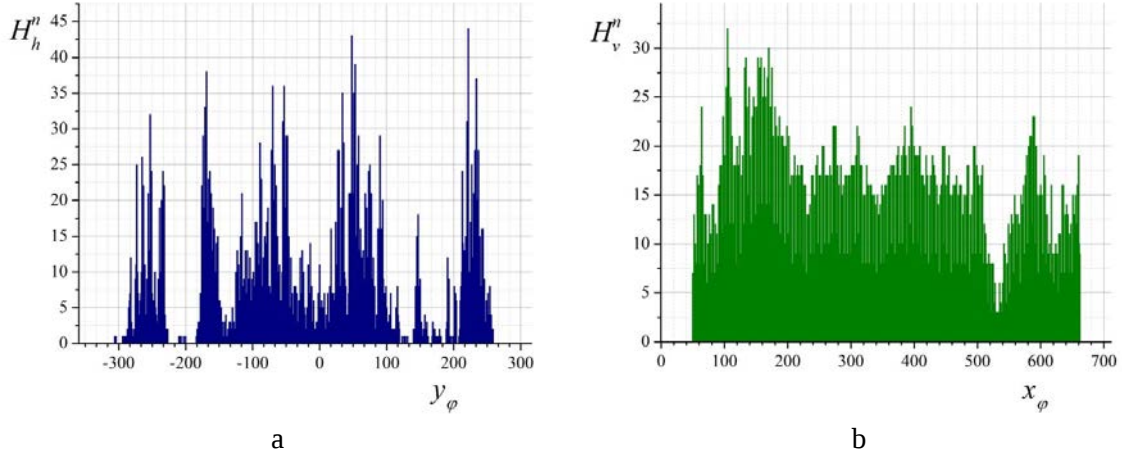


Figure 4: Normalised horizontal H_h^n (a) and vertical H_v^n (b) histograms for the image of the polycrystalline fatigue sensor surface

Each element of the histogram contains a number of pixels, which correspond to the objects of the ordered relief structures in a certain direction of the image analysed. The histogram functions contain the basic information about the distribution of the ordered structures along the coordinate axes of the image [8].

The normalised histograms for the image of the polycrystalline aluminum fatigue sensor surface (Fig. 1,b) are shown in Fig. 4. It should be noted that the horizontal histogram is characterised by the clearly defined peaks, which correspond to blocks of the elongated relief elements. At the same time, the vertical histogram is characterised by a much more uniform shape, which indicates the absence of the clearly defined linear elements in this direction.

The quantitative evaluation of the histogram view (8) was performed based on the spectral analysis of its functions. Using the fast Fourier transformation the histogram functions were presented in the form of the row:

$$H_h^n(y^\varphi) \approx \sum_{k=0}^{K_h} A_{hk} \cos\left(2\pi \frac{k}{n} y^\varphi - \vartheta_h\right), \quad H_v^n(x^\varphi) \approx \sum_{k=0}^{K_v} A_{vk} \cos\left(2\pi \frac{k}{m} x^\varphi - \vartheta_v\right) \quad (10)$$

The number of harmonics of the K_h, K_v array was chosen in such a way as to ensure that the accuracy of presenting the histogram function in the form of the sum of harmonics was not below the limit value of ε .

$$\left| H_h^n(y^\varphi) - \sum_{k=0}^{K_h} A_{hk} \cos\left(2\pi \frac{k}{n} y^\varphi - \vartheta_h\right) \right| \leq \varepsilon, \quad \left| H_v^n(x^\varphi) - \sum_{k=0}^{K_v} A_{vk} \cos\left(2\pi \frac{k}{m} x^\varphi - \vartheta_v\right) \right| \leq \varepsilon \quad (11)$$

The mean amplitudes of the spectrum of functions of the horizontal and vertical histograms A_{ah}, A_{av} were chosen as the informative parameters:

$$A_{ah} = \frac{1}{K_h} \sum_{k=0}^{K_h} A_{hk}, \quad A_{av} = \frac{1}{K_v} \sum_{k=0}^{K_v} A_{vk} \quad (12)$$

The mean amplitude of the spectrum allows for the quantitative evaluation of the surface relief elements orientation along the image axes. Its higher values correspond to the greater degree of damage along the given axis. So, by comparing the values of A_{ah} and A_{av} it is also possible to obtain information about the prevailing direction of propagation of surface defects.

The availability of the pair of generalized characteristics – mean gradients G_h , G_v and mean spectrum amplitudes A_{ah} , A_{av} – allows obtaining the complex integrated characteristic of the analysed image in two mutually perpendicular coordinate directions [9].

4. Summary

The algorithm for the integral evaluation of the surface condition is proposed, which allows determining the condition of the deformation relief under regular and programmed loading, and the main regularities in its evolution.

For the quantitative evaluation of the surface condition it is proposed to use a multitude of integral parameters: the general area of damage, mean gradient along the coordinate axes, and the mean amplitude of the histogram function spectrum.

Determining the main regularities in the fatigue damage accumulation allowed obtaining new data on localisation of plastic strain in the fatigue sensor, which provides for an increased accuracy of evaluation of the aircraft structure condition.

5. References

- [1] V.A. Romanova, R.R. Balokhonov, S. Schmauder, *Materials Science and Engineering A*. 564. (2013) 55.
- [2] M. Karuskevich, O. Karuskevich, T. Maslak, S. Schepak, *International Journal of Fatigue*. 39 (2012) 116.
- [3] P.V. Makarov, V.A. Romanova, *Theoretical and Applied Fracture Mechanics* 33(1) (2000) 1.
- [4] P.O. Maruschak, V.S. Mocharskyi, I.M. Zakiev, Yu.M. Nikiforov, *Proc. of the Int. conf. on Oxide Materials for Electronic Engineering (September 3-7)*, Lviv: NU Lvivska Politechnika, 2012.
- [5] I. Konovalenko, P. Maruschak, *Proc. of the Int. conf. on Modern Problems of Radio Engineering Telecommunications and Computer Science (TCSET)*, IEEE, 2012.
- [6] R.O. Duda, P.E. Hart, *Artificial Intelligence Center, Comm. ACM*, 15 (1972) 11.
- [7] P.O. Maruschak, S.V. Panin, S.R. Ignatovich, et al, *Theoretical and Applied Fracture Mechanics*. 57 (2012) 43.
- [8] I.V. Konovalenko, P.O. Marushchak, *Optoelectronics, Instrumentation and Data Processing*. 47 (2011) 360.
- [9] P.O. Yasnii, P.O. Marushchak, I.V. Konovalenko, R.T. Bishchak, *Materials Science*. 44 (2008) 833.